Comet Halley: Investigations, Results, Interpretations
ed: J. W. Mason ~~and F. L. Whipple~~, Ellis Horwood, New York, 1990, V.1, p.147

9

Some results of neutral and charged particle measurements in the vicinity of comet Halley by Vega-1, 2 spacecraft

K. I. Gringauz and M. I. Verigin

1 INTRODUCTION

Both Vega-1 and Vega-2 spacecraft carried plasma instrument scientific packages PLASMAG-1 which included neutral particle flux sensors and ion and electron energy spectrometers†

Two hemispherical electrostatic analyzers measured the energy/charge spectra of ions arriving from the spacecraft–comet relative velocity direction (the Cometary Ram Analyzer CRA) and from the direction of the Sun (the Solar Direction Analyzer SDA). Electrons were measured by a cylindrical electrostatic analyzer (EA) which was orientated perpendicular to the ecliptic plane. PLASMAG-1 also included two Faraday cups. The Solar Direction Faraday Cup (SDFC) measured the solar wind ion fluxes, while the Ram Faraday Cup (RFC), in addition to measuring the total flux of ions arriving from the ram direction, provided information on the neutral particle flux from the comet by detecting the secondary electrons and ions produced by the neutrals striking a metallic collector.

A description of the scientific payload and the detailed results of the plasma measurements have been published elsewhere (Apáthy *et al.* 1986, Balebanov *et al.* 1987, Galeev *et al.* 1986a, b, 1987, Gringauz *et al.* 1983, 1985, 1986a b, c, d, e, 1987a, b, Remizov *et al.*, Verigin *et al.* 1986, 1987a, b). The present paper, which is mainly a compilation of the above mentioned papers, contains the main observational results of the PLASMAG-1 scientific packages and our present understanding of these results.

† The package was developed in the Space Research Institute of the USSR Academy of Sciences and in the Central Research Institute for Physics of the Hungarian Academy of Sciences, with participation of the Max-Planck-Institut für Aeronomie (FRG).

2 THE NEUTRAL DENSITY DISTRIBUTION

The neutral particle density was estimated *in situ* aboard the Vega-1, 2 spacecraft by means of a rather primitive multi-electrode Ram Faraday Cup in a special mode of operation (Apáthy *et al.* 1986,

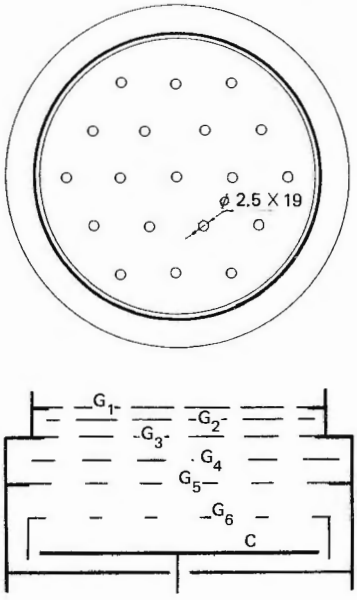

Fig. 1 — Schematics of the PLASMAG-1 Ram Faraday Cup (RFC) for measuring the neutral gas distribution in the vicinity of Halley's comet. The 19 holes in G_1 are of 2.5 mm diameter.

Comet Halley - investigations, results, interpretation v 1 plasma, gas
Ed , Ellis Horwood Publ Co , p 147 , 1990

Gringauz *et al.* 1983, 1985, 1986a, b, Remizov *et al.* 1986). Fig. 1 (Remizov *et al.* 1986) is a schematic of this sensor which is different from the Faraday cups traditionally used on space probes. To avoid damage to the grid by cometary dust, the analyzing grid system was substituted by a flat disk electrode system G_1–G_6. There were 19 holes on each disk and the diameter of the holes increased toward the collector C.

When neutral particle fluxes were measured, voltages of −40 V and +3500 V were applied to electrodes G_2 and G_4, respectively. Photo- and secondary electrons of the surrounding plasma with energies $E_e < 40$ eV, and cometary and solar wind ions of energies $E_i < 3500$ eV were thereby diverted from the collector by these potentials.

In this way the collector current I_c of the RFC is given by the following, in the vicinity of the comet:

$$I_c \approx I_{se} - I_{si} + I_{ph} - I_e \qquad (1)$$

where I_{se} and I_{si} are the secondary electron and sputtered ion currents, which are proportional to the flow of neutral particles (the individual short bursts in I_c are associated with the registration of dust particles), I_{ph} is the photoelectron current, and I_e is the current of energetic electrons reaching the collector. To register I_{se} and I_{si} separately, a potential of +40 V and −60 V was applied to electrode G_6, respectively. In the first case, when the current of secondary electrons is measured, I_{si} is suppressed, and I_c is determined by I_{se}, I_{ph}, and I_e, thus:

$$I_{ce} \approx I_{se} + I_{ph} - I_e \qquad (2)$$

In the second case, when the sputtered ions current is registered, I_{se} is suppressed, I_{ph} decreases significantly and changes its sign (this current is now not produced by photoelectrons originating from the collector, but by the photoelectrons originating from electrode G_6), and the current I_e slightly decreases since in this case only the electrons with energy $E_e > 60$ eV can reach the collector. Thus, the collector current (ions) is:

$$I_{ci} \approx -I_{si} - I_{ph} - I_e \qquad (3)$$

The following equation was used to determine the neutral gas density on the basis of the measured $I_{ce,i}$ values:

$$n_n = \frac{I_{ce,i} - I_o}{qV_{sc}SY_{e,i}} \qquad (4)$$

Here I_o is the sum of currents I_{ph} and I_e, q is the electron charge, $V_{sc} = 79.2$ km s^{-1} (76.8 km s^{-1}) is the velocity of Vega-1 (Vega-2) relative to the comet, $S = 0.93$ cm^2 is the total surface area of the holes of electrode G_1 (see Fig. 1), and $Y_{e,i}$ is the yield of secondary electrons and ions provided by neutral particles impacting the collector. In general, I_o in equation (4) is not a constant, as it will depend on time and on the distance from the cometary nucleus. However, for the estimation of n_n we assumed I_o = constant and used the value as measured by RFC at large distances from the comet, where $I_{se,i} \approx 0$.

The accuracy of n_n estimations based on RFC data in the regions where $I_{ce,i} \gg I_o$ depends mainly on our present knowledge of the secondary electron Y_e and sputtered ion Y_i yields from the Ni emitter (collector) used. The secondary electron emission from the metal surface may be caused in two ways (Kaminsky 1965). The potential emission occurs when the impinging particle is an ion or an excited neutral. There is no minimum kinetic energy to start this process, but the influence of it on the I_{ce} value is small, as the number of ions with $E_i > 3500$ eV and the number of excited neutrals is small relative to the number of neutrals in the ground state. The kinetic electron emission occurs as a result of the energies of impinging particles exceeding the threshold energy. For the water group neutrals this energy is close to their energy relative to the spacecraft. Finally, the secondary ion emission results from the thermal sputtering of metal by a localized heating process.

There are no direct experimental data on $Y_{e,i}$ for Ni targets bombarded with water group molecules with $V_{sc} \approx 80$ km s^{-1}. Fig. 2 presents the results of measurements of $Y_{e,i}$ dependence on energy for Al and Au targets bombarded by water molecules (Shmidt & Azens 1987). These measurements were conducted with energies greater than ~700eV while the energy of water group molecules relative to the spacecraft is ~500 eV. The $Y_e \approx 0.3$ and $Y_i \approx 0.005$ values which were used during the preliminary processing of the RFC data are marked in Fig. 2 by asterisks.

The yield values presented in Fig. 2 were chosen by the PLASMAG-1 team just after receiving the first RFC cometary flyby data on 6 March 1986, and Fig. 3 (Gringauz *et al.* 1986b) (computed from expression (4) and $Y_{e,i}$) was presented to the scientific community

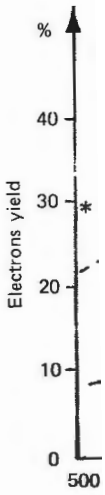

Fig. 2 — Yields of seconc
RFC measurements pro

meeting on the nex
as providing a reas
imental data avail
providing the cont
profile n_n (R) (Fig

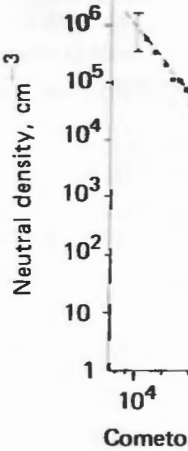

Fig. 3 — Radial profi
measured inbound by th
with the distribution p
ionization scale length o
rate of $Q_o \sim 1.3 \times 10^{30}$

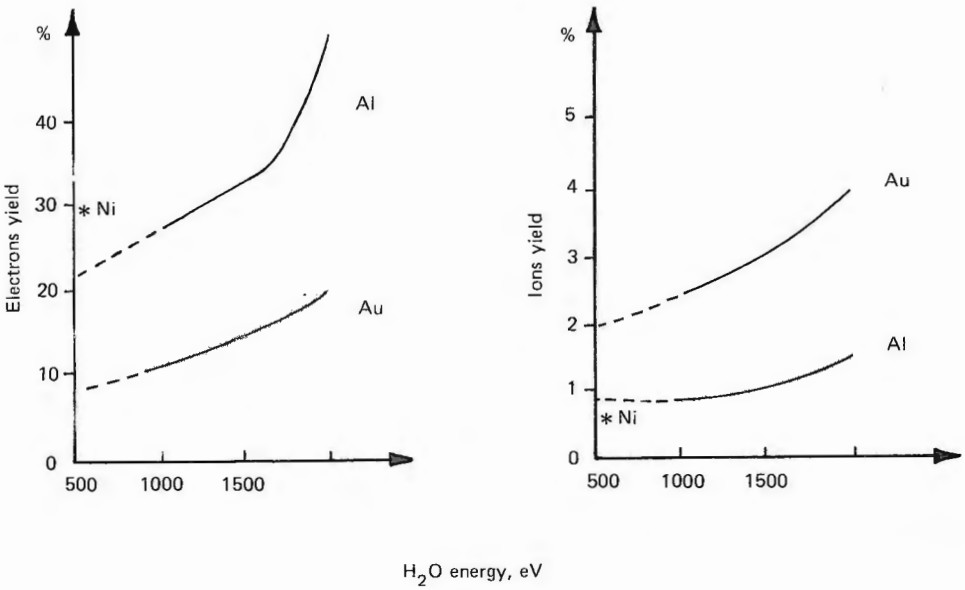

Fig. 2 — Yields of secondary electrons and sputtered ions from Al and Au targets (Shmidt & Azens 1987) compared with the values used for RFC measurements processing (asterisks).

meeting on the next day. Both $Y_{e,i}$ values were chosen as providing a reasonable agreement with the experimental data available (Fig. 2), and simultaneously providing the continuity of the neutral gas density profile n_n (R) (Fig. 3) as a function of R at the cometocentric distances $R \approx 10^5$ km, where the secondary electron registration mode is replaced by the sputtered ion registration mode. The optimization analysis of $Y_{e,i}$ selection is not yet completed, so the profile presented should be considered as preliminary; we evaluate its uncertainty to be a factor of ≈ 2.

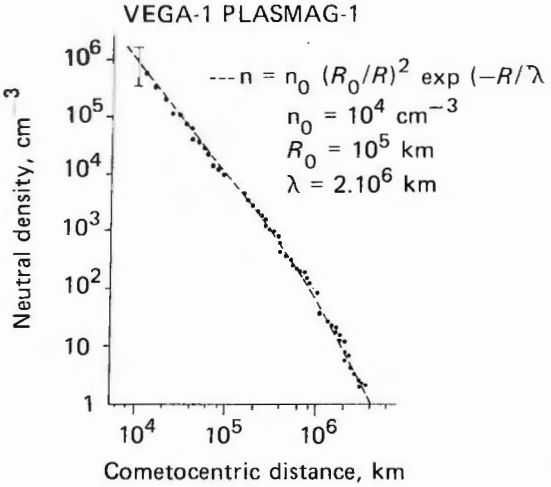

Fig. 3 — Radial profile of the overall neutral gas density, as measured inbound by the Vega-1 Ram Faraday Cup. Comparison with the distribution predicted by theory (dotted line) yields an ionization scale length of $\lambda \sim 2 \times 10^6$ km and an overall production rate of $Q_o \sim 1.3 \times 10^{30}$ molecules s^{-1}.

In addition to the n_n (R) profile, the dashed line in Fig. 3 represents a simple fit to the data, assuming R^{-2} $\exp(-R/\lambda)$ density dependence. The ionization scale length was estimated to be $\lambda \approx 2 \times 10^6$ km, and a value of $\approx 1.3 \times 10^{30}$ molecules s^{-1} was obtained for the total gas production rate Q_o.

The data shown in Fig. 3 were obtained during the inbound pass of the flyby. On the inbound leg of Vega-2, the estimated n_n values were half those for Vega-1 at distances 1.5×10^4 km $< R < 10^5$ km, although the n_n values estimated from the data on both spacecraft are significantly closer to each other further away from the nucleus. Moreover, the values of n_n estimated from the I_{ce} measurements on the outbound leg of both Vega-1 and Vega-2 at distances 1.5×10^5 km $< R < 3 \times 10^5$ km are about half the corresponding n_n values on the inbound leg (see Figs. 4, 5 in Remizov *et al.* 1986).

These and other deviations might be caused by jets of neutral gas originating from the rotating nucleus.

Also, (1) the solar UV radiation scattered by the comet may have some influence on the instrument performance, and (2) the solar radiation pressure can influence the asymmetry of the neutral gas distribution along the spacecraft trajectory. Although the neutral gas density estimations presented above were produced on the basis of a very simple instrument, the gas production rate of Halley's comet estimated from the RFC observations on board Vega-1 and Vega-2 is in reasonable agreement with the estimates provided by other instruments on board Vega-1, Vega-2, and Giotto. The production rates for the H_2O and OH molecules were determined as $Q_{H_2O} \approx 4 \times 10^{29}$ s^{-1} and $Q_{OH} \approx 1.7 \times 10^{30}$ s^{-1} from the spectroscopic observations by the three-channel spectrometer (TKS) on board Vega-2 in the visible and infrared spectral ranges (Krasnopolsky *et al.* 1986), and as $Q_{OH} \approx 9 \times 10^{29}$ s^{-1} in the near ultraviolet range (Moreels *et al.* 1986). The value of Q_o estimated from the data measured by PID onboard Vega-1 varies between $10^{30} < Q_o < 4 \times 10^{30}$ s^{-1} at cometocentric distances $R < 1.5 \times 10^5$ km.

Finally, a preliminary estimate of the gas production rate of $Q_o \approx 6.9 \times 10^{29}$ s^{-1} was provided by the instrument NMS on board Giotto (Krankowsky *et al.* 1986). Besides, at cometocentric distances 2×10^5 km $< R < 3 \times 10^6$, the RFC was the only sensor on spacecraft that was able to measure the distribution of neutral gas along the trajectory.

3 COMETARY PLASMA PHENOMENA

The main feature of near cometary space is the increase, by orders of magnitude, of the population of neutral particles with approach to the nucleus of the comet, as considered above. This phenomenon determines the peculiarities of plasma flow in this region.

The plasma sensors of the PLASMAG-1 scientific package are shown schematically in Fig. 4 (Apáthy *et al.* 1986). The essential feature of the CRA and SDA analyzers, is the quadrupole electrostatic lenses in front of curved analyzing plates. These lenses increase the fields of view of the CRA and SDA up to 14° × 32° and 30° × 38°, respectively. The number of grids in the SDFC is the same as the number of flat electrodes in the RFC (Fig. 1). For the ion flux measurements, the voltages −40 V and −60 V were applied to the electrodes G_2 and G_6. Then the subtraction of

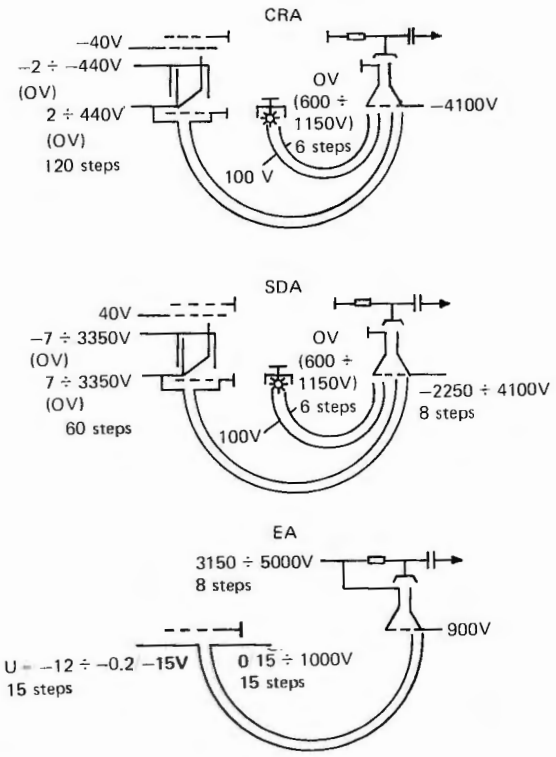

Fig. 4 — Schematics of the PLASMAG instrument.

collector C currents, measured with voltages 0 V and 3500 V applied to the G_4 electrode, permits the evaluation of the net ion flux fed to the SDFC and RFC. A more detailed description of the instrumentation is given in Apáthy (1986) and Gringauz *et al.* (1983, 1986a).

For convenience of further discussion of near-cometary plasma phenomena we present first, in Fig. 5, a general overview of the different plasma formations, as identified from the PLASMAG-1 plasma observations on board Vega-1 and -2 during their encounter with comet Halley (Gringauz *et al.* 1985). The terms 'cometosheath' and 'cometopause', were introduced by the PLASMAG-1 team (Gringauz *et al.* 1986b) to indicate the principal difference with respect to the physical processes occurring over this cometary regions as compared to those observed in the magnetosheath of planets with strong intrinsic magnetic fields, or in the ionosheath of planets with intense gravitational fields. These terms are now generally accepted. Let us consider the peculiarities of

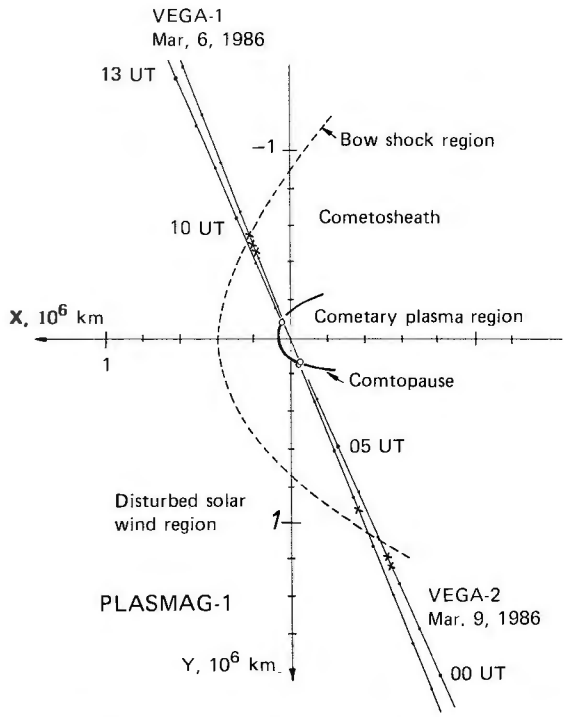

Fig. 5 — General overview of the inbound and outbound locations of the 'bow shock' and of the 'cometopause' as well as of the 'cometosheath' and of the 'cometary plasma region', as identified from PLASMAG-1 plasma observations on board Vega-1 and -2 during their encounter with comet Halley.

the plasma flow within the different plasma formations, beginning from the outermost ones.

3.1 Solar wind region disturbed by picked-up ions and the bow shock

In Fig. 6 the decrease in the solar wind proton velocities with cometocentric distance R is shown, as measured by the SDA on both Vega-1 and Vega-2 during their inbound legs. (Verigin *et al.* 1986, 1987a). The location of the bow shock, which was determined from simultaneous measurements of the plasma, the plasma waves, and of the magnetic field (Galeev *et al.* 1986a) is marked by S. As one can see, the decrease of the solar wind velocity due to mass loading by heavy cometary ions had already started at a distance of 2–3 $\times$ 10^6 km from the nucleus, i.e. 1–2 $\times$ 10^6 km upstream of the bow shock.

The process of mass loading and deceleration of the solar wind by new ions, originating from the cometary neutrals, is well known in principle, and has already been considered in a number of hydrodynamic models of solar wind interaction with comets (see, e.g. Shmidt & Wegmann 1982). These ions first form a ring distribution in velocity space. The Alfvén wave turbulence being excited by the ion-cyclotron instability of such a distribution isotropizes the newly formed ions in the coordinate system moving with the solar wind (Sagdeev *et al.* 1986).

On the basis of the kinetic theory developed in that paper, a complete system of equations for the variation of the isotropic part of cometary ion distribution function and the hydrodynamical parameters of the flow along the X axis (parallel to the solar wind direction) was presented and solved in Galeev (1986, 1987) and Galeev *et al.* (1986a). In a three-dimensional case, if the main contribution to the plasma pressure P comes from the cometary ions with average mass $m_i \approx 17\, m_p$, the hydrodynamic part of this system can be written in the following form:

$$\left.\begin{aligned} \operatorname{div}(\rho V) &= Q(R) \\ \rho(v, \nabla)V &= -\nabla P - Q(R)V \\ \operatorname{div}(PV) &= QV^2/2, \end{aligned}\right\} \qquad (5)$$

where ρ and $\mathbf{V}$ are the plasma flow density and velocity, and $Q = m_i n_n v_n/\lambda$ is the mass loading rate.

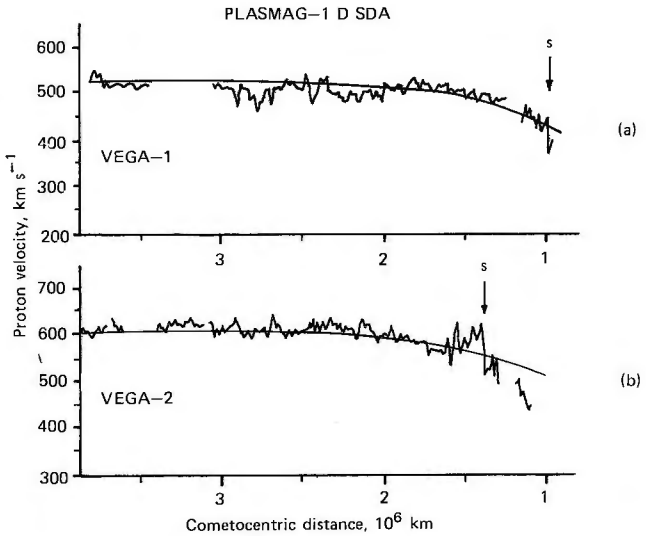

Fig. 6 — Radial dependence of the solar wind bulk velocity, as observed by Vega-1 and Vega-2 on their inbound trajectories upstream of the bow shock of Comet Halley (marked by S).

From equations (5) one can obtain the expected variation of the flow parameters along the Vega-1, -2 trajectories at large cometocentric distances, where the initial velocity u_o and density ρ_o are slightly perturbed by the cometary ions:

$$u = u_o - \frac{4}{3\rho_o} L_o(R, \varphi),$$

$$v = \frac{\cos\varphi.\sin\varphi}{3\rho_o} L_2(R, \varphi),$$

$$\rho = \rho_o + \frac{1}{u_o}\left(2L_o + \frac{3\cos^2\varphi - 1}{6} L_2 + \frac{\cos^2\varphi.\sin^2\varphi}{2} L_4\right),$$

$$P = \frac{u_o}{3} L_o(R, \varphi) \qquad (6)$$

where,

$$L_n(R, \varphi) = R \int_{\cos\varphi}^{\infty} Q(R\sqrt{\zeta^2 + \sin^2\varphi})\zeta^n \, d\zeta,$$

u and v are parallel and perpendicular to X axis components of the plasma flow velocity vector, and $\phi \approx 110°$ is the angle between this axis and the Vega-1, 2 trajectory.

The cometocentric dependence of $V(R) \approx u(R)$ computed in accordance with (6) along the Vega-1, 2 trajectories, is shown in Fig. 6a (u_o = 540 km s^{-1}) and in Fig. 6b (u_o = 620 km s^{-1}) by smooth curves. The neutral density profile $n_n(R)$ was used in accordance with the RFC data described in the previous section; the initial ρ_o values were based on SDA measurements onboard Vega-1 ($\rho_o/m_p \approx 12$ cm^{-3}) and Vega-2 ($\rho_o/m_p \approx 11$ cm^{-3}). The reasonable agreement between the computed and measured velocity profiles is obvious.

The plasma flow deceleration while approaching the cometary nucleus is not continuous, and the bow shock is formed in front of the comet as a result of increasing mass loading by heavy cometary ions. The bow shock positions observed by Vega-1,2 are shown by crosses in Fig. 5. Fig. 7 (Verigin *et al.* 1986, 1987a) presents the energy spectra measured by the SDA onboard Vega-1 when crossing the bow shock on the inbound leg and on the outbound leg. Also, the gradual slowing down of protons, and a gradual widening of the energy spectra, can be observed when approaching the comet, i.e. the ion temperature is increasing several hours before reaching the bow shock. After a data gap of 20 minutes around 0300 UT, the ion temperature was already so high that the proton distribution overlaps the α particle peak in the spectrum. The gradient of the velocity is increasing significantly when crossing the bow shock at a distance of 1.02 × 10^5 km from the nucleus (~0346 UT).

The variation of the plasma parameters seems to be more complicated when crossing the bow shock on the outbound leg of Vega-1. The highest gradient in the plasma velocity was observed between 0900 and 0930 UT at a distance of about 5.5 × 10^5 km from the nucleus. At the same time the ion temperature stayed high, so that the α peak could not be distinguished from the proton distribution until 1130 UT (R = 1.2 × 10^6 km). Thus, on the outbound leg the bow shock was crossed at a distance of 5.5 ± 1 × 10^5 km (Galeev *et al.* 1986a), and the high ion temperature which can be observed until 1220 UT for about another 8 × 10^5 km is associated with the high lever of magnetohydrodynamic (MHD) activity in the foreshock region.

The latter distance seems to be determined only by the distribution of the neutral gas density n_n around Halley's comet. The increase of n_n to 30 cm^{-3} at a distance of 1.3 × 10^6 km from the nucleus (Gringauz *et al.* 1985, 1986b, Remizov *et al.* 1986) seems to be enough to ensure turbulent heating of the solar wind ions caused by the unstable beam-like distribution of ions of cometary origin. The location of the bow shock

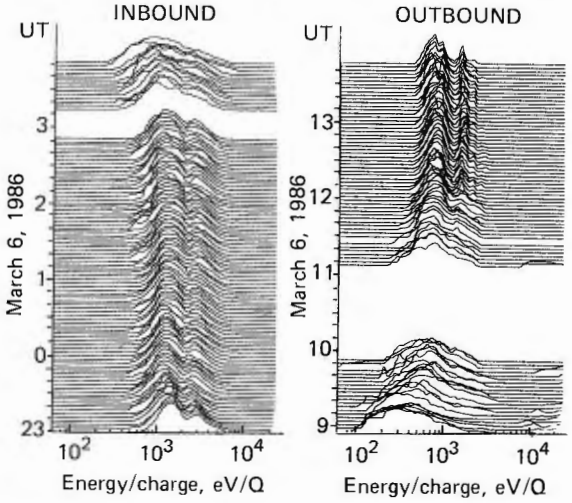

Fig. 7 — Ion energy spectra measured by Vega-1 on the inbound leg and on the outbound leg around the bow shock of Halley's comet.

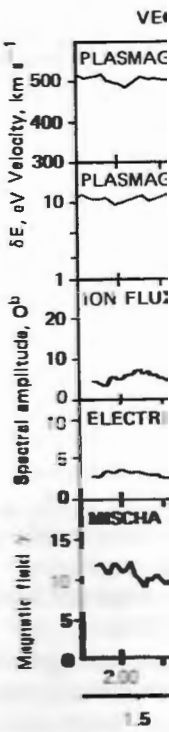

Fig. 8 — The b
inbound bow shoc
1986. From top
temperature meas
flux fluctuations
f = 1.5 Hz; magn

and the gradi
shock is natu
compared to th
as seen in Fig
around the fla
subsolar point
for the differ
regions of ho
outbound arou

The behavi
the bow shock
in Fig. 8 (Gale
and the effecti
first and the
spectra, respe
pendicular bo
sharp increase
lower hybrid p

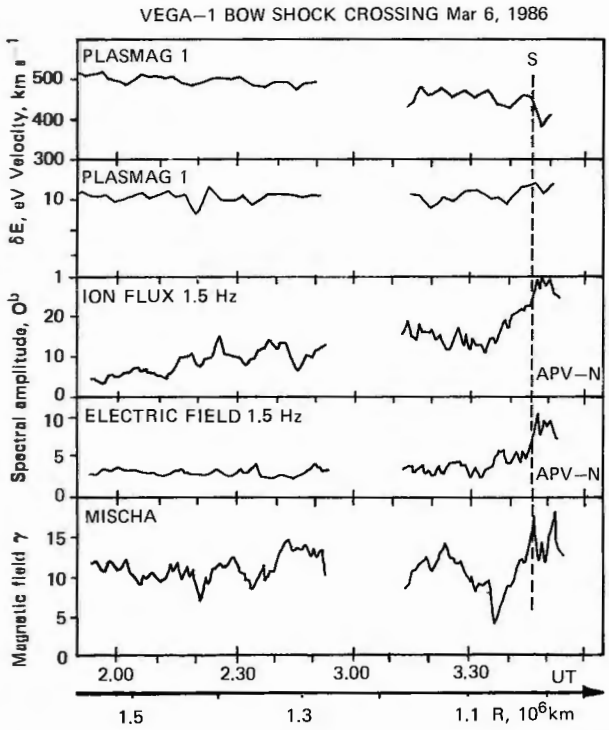

Fig. 8 — The behaviour of solar wind parameters during the inbound bow shock crossing by the Vega-1 spacecraft on 6 March 1986. From top to bottom: solar wind velocity and effective temperature measured in solar direction; spectral amplitude of ion flux fluctuations and electric field oscillations with the frequency $f = 1.5$ Hz; magnetic field strength.

and the gradient of the ion velocity related to the shock is naturally different on the inbound leg as compared to the outbound leg of the Vega-1 trajectory as seen in Fig. 5, since the bow shock was crossed around the flanks on the inbound leg but closer to the subsolar point on the outbound leg. This is the reason for the difference between the dimensions of the regions of hot solar wind observed inbound and outbound around the bow shock.

The behaviour of other plasma parameters across the bow shocks can be judged from the data presented in Fig. 8 (Galeev *et al.* 1986a). The solar wind velocity and the effective temperature δE on this figure are the first and the second moments of SDA ion energy spectra, respectively. The crossing of this quasiperpendicular bow shock is identified most easily by the sharp increase in intensity of the plasma waves. These lower hybrid plasma waves are excited by the beam of cometary ions leaking forward from behind the subshock front, similar to the excitation of these waves at the quasiperpendicular Earth bow shock by the beam of protons reflected from the shock (Galeev 1987). The jump of the magnetic field at the shock front is masked in Fig. 8 by the strong MHD turbulence of a loaded solar wind.

The more complicated phenomena were seen at the quasi-parallel cometary shocks observed by Vega-1 on the outbound leg (Fig. 7) and by Vega-2 on the inbound leg of the trajectory (Galeev *et al.* 1986a). Further study and comparison with computer simulations of these formations (Galeev 1987) is required.

3.2 Cometosheath region and the cometopause

Downstream of the cometary bow shock both Vega spacecraft encountered a region which was called the cometosheath (Gringauz *et al.* 1986b). The principal difference between the plasma flow within this region and that within the regions downstream of bow

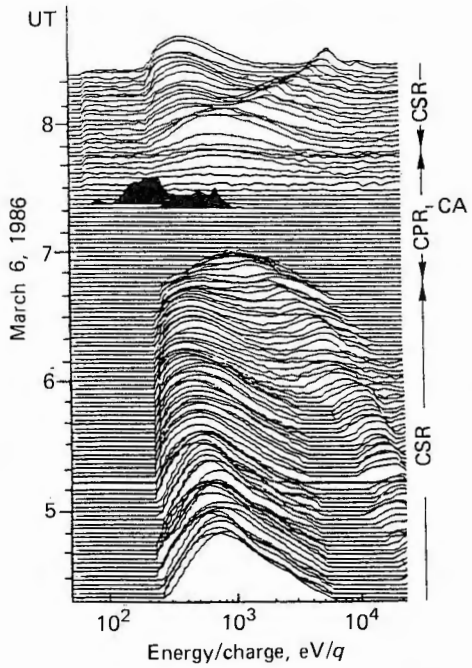

Fig. 9 — Sequence of energy-per-charge spectra observed by the solar-direction ion electrostatic analyzer SDA on board Vega-1: (a) on the inbound and outbound leg in the cometosheath regions (CSR) and in the cometary plasma region (CPR).

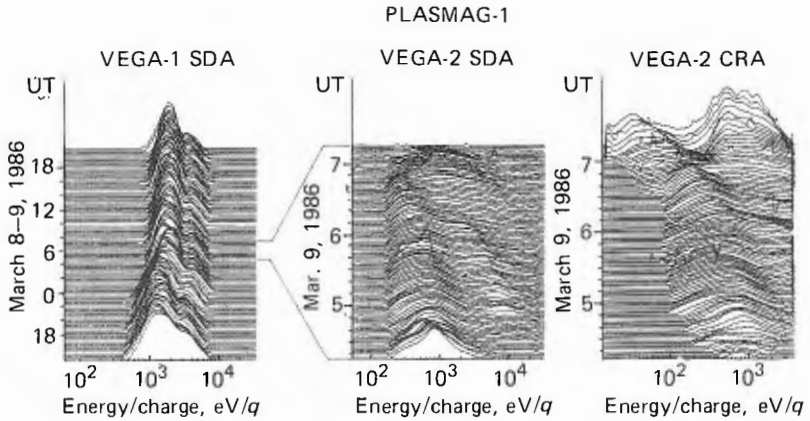

Fig. 10 — Sequences of ion spectra measured (a) by the Vega-1 SDA in the solar wind during the time of the encounter of Vega-2; (b) by the Vega-2 SDA downstream of the cometary bow shock and up to a cometocentric distance of $\sim 1.5 \times 10^4$ km; and (c) by the Vega-2 Cometary Ram Analyzer (CRA) over the same distance range.

shocks near other celestial bodies is readily seen from the ion spectra as measured by the Vega-1 SDA (Fig. 9) and by the Vega-2 SDA (Fig. 10b) and CRA (Fig. 10c) over the cometosheath. It is worth noting that the comparison of the ion spectra observed by the Vega-1 SDA (Fig. 10a) in the undisturbed solar wind and, simultaneously, by the Vega-2 SDA (Fig. 10b) in the cometosheath region certainly proves that the plasma disturbances in this region are not of solar wind origin.

At a cometocentric distance of $\sim 8 \times 10^5$ km the SDA post-bow shock ion spectra are characterized by a wide, single maximum distribution of decelerated and heated solar wind ions (see the lower parts of Figs 9 and 10b). The proton bulk velocity is 350–400 km s^{-1}. Approaching the nucleus, the following are observed: (1) the direction of the solar wind bulk flow changes smoothly from the solar toward the ram direction, as the maximum intensities at the same energies gradually decrease (increase) in the SDA (CRA), respectively (Fig. 10b, c); (2) the bulk velocity of the solar wind and its temperature gradually decrease (Fig. 9, 10b, c); (3) a second maximum starts to appear in the SDA spectra at higher energies (Fig. 9), indicating that the corresponding ions may initially have had energies larger than 25 keV, which are not observable by the SDA. Certainly, these latter ions must be of cometary origin. Comparing the energies at the two peaks in the ion spectra, it is reasonable to deduce that these ions originate from the water-group (O^+, OH^+, H_2O^+, H_3O^+).

As was noted above, after a few cyclotron periods newly created cometary ions are isotropized in the coordinate system moving with the solar wind (Sagdeev *et al.* 1986). In this way the newly created ions are arriving from the solar direction with a maximum energy $4m_i/m_p$ times higher than the proton energy, independently of the angle between the solar wind flow and the magnetic field direction.

In the solar wind upstream of the bow shock, the energy of these heavy ions exceeds the upper limit of the energy range of the SDA ($E_i/q < 25$ keV). But in the outer regions of the cometosheath, where the solar wind flow is already decelerated by the shock and by the mass-loading process, the SDA measurements are in reasonable accordance with the abovementioned process of implantation of cometary ions into the plasma flow at large distances from the comet (Verigin *et al.* 1986, 1987a).

With deeper penetration into the cometosheath, the proton energy gradually decreases. The energy of the cometary ions observed in the SDA decreases faster, so that the ratio of the energy of heavy ions to the energy of protons is also decreasing (Fig. 9). At distances of 3–4 $\times 10^5$ km from the nucleus (0600–0615 UT) the velocity of cometary ions from the solar direction decreases to the value of the proton velocity, owing to some collective process, which is not fully

understood. Also, the fluxes of these two populations become comparable. Later, the rate of energy decrease increases further for the heavy ions, while the energy of the protons practically ceases to change.

Around the cometopause (~0645 UT), which separates the cometosheath from the cometary plasma region, solar wind protons disappear from the acceptance angle of the SDA, and cometary ions produce a peak around 1 keV in the energy spectrum (Figs 9, 10b). When the velocity of Vega-1,2 relative to the comet is taken into account, the velocity of the heavy ions relative to the comet can be estimated to be a few tens of kilometres per second in the vicinity of the cometopause, while the proton velocity is still around 200 km s^{-1} in this region.

After closest approach (CA in Fig. 9) these characteristic changes in the cometosheath plasma occur again on the outbound leg, but in reverse order.

The energy spectra of cometary ions as measured by PLASMAG-1 in the inner region of the cometosheath might be interpreted in two different ways. Here, the ratio of the energy of cometary ions $E^1{}_i$ to the proton energy E_p measured by the SDA is smaller than $4m_i/m_p$ (~60–80), and it gradually decreases with decreasing cometocentric distances. The IIS (implanted ion sensor) of the JPA instrument on board Giotto was able to measure ions up to energies of $E_i/q < 90$ keV and to estimate the mass of the ions (Johnstone *et al.* 1986). According to the measurements of IIS there is another more energetic branch in the energy spectrum corresponding to water group ions with an energy of $E^2{}_i \approx 4m_i/m_pE_p$ as well as the branch which was also observed by the SDA. If the ratio $E^2{}_i/E_p \approx 4m_i/m_p$ is constant in the cometosheath, the ions with energies $E^2{}_i$ might have been locally ionized and picked up by the process discussed above. In this case, the ions observed by the SDA with energies $E^1{}_i < E^2{}_i$ might have been ionized further upstream of the population with energies $E^2{}_i$, and they might have lost their energy because of some later collective processes (Gringauz *et al.* 1985).

However, there is a preferable explanation for the existence of these two different cometary ion populations: the ions with the energy $E^2{}_i$ were actually created far upstream from the point of observation (Johnstone *et al.* 1986, Verigin *et al.* 1987a), but the proton energy slightly changes in the cometosheath as observed by the SDA. Hence the ratio $E^2{}_i/E_p$ does not change much, or stays almost constant, as in the first case. The ions registered with energies $E^1{}_i$ were created in the vicinity of the spacecraft. First, these ions are only partly taken into the solar wind flow; however, when approaching the cometopause, these ions are no longer a minor population. At the start of this process there is no complete isotropization in the coordinate system moving with the solar wind. But when approaching the cometopause, the density of these ions (Fig. 9) is increasing, thus the energy of the solar wind flow will not be large enough to increase the velocity of all the newly created heavy ions. In the vicinity of the cometopause these ions are accelerated only to a velocity of a few tens of kilometres per second. Since the spacecraft has a velocity of ~80 km s^{-1} relative to the comet, the slowly moving newly created cometary ions will be observed by the SDA with an energy of about 1 keV around the cometopause. There is an additional fact in favour of the possibility that the cometary ions belonging to the less energetic branch $E^1{}_i$ were created not very far from the spacecraft: the flux of these ions increases with decreasing R (see Fig. 9), corresponding to the increase in the neutral gas density. The fluxes of heavy ions, however, belonging to the high-energy branch do not increase significantly when approaching the nucleus (see Fig.2 of Johnstone *et al.* (1986).

The characteristic feature of the electron plasma component in the cometosheath is a decrease of electron temperature T_e with approach to the cometopause. From the data presented in Fig. 11 (Gringauz

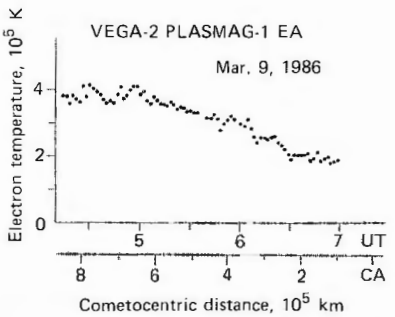

Fig. 11 — Distribution of the electron temperature in the cometosheath of comet Halley between 8 × 10^5 and 1.6 × 10^5 km (cometopause). CA = closest approach.

et al. 1986e, 1987a) it readily follows (1) that there is an overall decrease of T_e from about 4×10^5 K to about 2×10^5 K within this region; (2) that T_e decreases fastest within the region of about 5.5–6 $\times 10^5$ km, but stays approximately constant outside; and (3) that there are significant fluctuations in T_e in the region outside about 6×10^5 km. It should be mentioned that at a cometocentric distance of about 5–6 $\times 10^6$ km, i.e. in the undisturbed solar wind, the electron temperature was about 2×10^5 K, and that it had already increased to its maximum value of about 3.5–4 $\times 10^5$ K, at a distance of about 3×10^5 km upstream of the cometary bow shock.

During the encounter of the Giotto spacecraft with comet Halley, electrons were measured by the electron electrostatic analyzer EESA of the RPA experiment (Rème *et al.* 1986). In the undisturbed solar wind the electron temperature was about 2.5×10^5K and it occasionally increased to about 3.5×10^5K beyond 10^5 km upstream of the bow shock. Downstream, in the region from 1.15×10^6 km to 5.5×10^5 km, T_e stayed practically constant (3.5×10^5 K) but with large fluctuations superimposed, while afterwards, when approaching the cometopause, T_e decreased to about 2×10^5 K. Thus, outside the cometopause both the Vega-2 and Giotto electron measurements are in excellent agreement, not only with respect to the actual values of T_e but also with respect to its overall radial dependence.

We propose that the decrease in electron temperature from about 4×10^5 K near the bow shock to about 2×10^5 K at the cometopause, as observed by Vega-2 and Giotto independently, is due to inelastic collisions between the thermal electrons and the cometary neutral gas (Gringauz *et al.* 1986e, 1987a). Near the cometopause at $R \approx 1.6 \times 10^5$ km the neutral density is about $n_o \approx 5 \times 10^3$ cm^{-3} (Remizov *et al.* 1986). The energy loss of electrons caused by inelastic collisions with neutrals of the water group is $N_o L_o \approx 2 \times 10^{-11}$ eV cm^{-1}, where $L_o \approx 4 \times 10^{-15}$ eV cm^2 is the energy loss function for electrons with an energy of about 40 eV (Olivero *et al.* 1972), and N_o is the number density of neutrals of the water group. The plasma velocity near the cometopause is $V \approx 200$ km s^{-1} (Galeev *et al.* 1987). The characteristic time for the plasma flow through the cometopause is therefore $\tau \approx 2R/V \approx 1.5 \times 10^3$ s (taking into account that $\phi \approx$ 110°). During this time the thermal electrons, with an average velocity of about 4 000 km s^{-1}, have traversed a distance of about 6×10^6 km. Thus, according to the above estimate, their energy loss is about 12 eV.

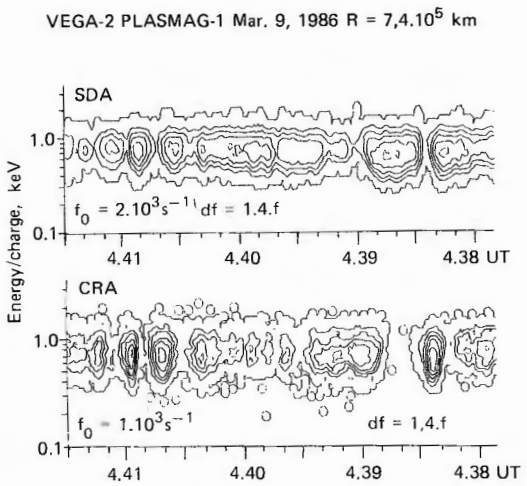

Fig. 12 — Spectrograms of the ion fluxes as observed by the Sun-directed (SDA) and ram-directed (CRA) ion electrostatic analyzer on board Vega-2 simultaneously in the cometosheath. Note the variations in the direction of the plasma flow of cometary ions.

As well as the large-scale changes in the plasma flow in the cometosheath, which determine the global picture of the solar wind flowing around the comet, a high level of MHD turbulence with a wide frequency range is characteristic for this region. An example of the variations in the direction of the plasma flow within the cometosheath is presented in Fig. 12 (Verigin *et al.* 1986, 1987a). In these spectrograms, registered by the CRA and the SDA at a distance of about $R \approx 7.4 \times 10^5$ km from the nucleus, the characteristic duration of the variations is 20–30 s. The outermost isolines correspond to a counting rate of f_o, and each inner isoline represents a counting rate which is 1.4 times greater than the corresponding value of the adjacent outer line. The variations in the flow intensity observed by both analyzers are caused by variations in the direction of the ion flow. When the intensity of the ion flow decreases in the direction of the CRA analyzer, the counting rates observed by the SDA increase simultaneously, and vice versa. The approximate value of this declination of the proton flow from the original direction can be estimated as

$$\delta\alpha \approx \frac{2\kappa T}{m_i V^2} \cdot \ln\left(\frac{N_{max}}{N_{min}}\right) \approx 5^\circ \qquad (7)$$

where the proton temperature is $T \approx 3 \times 10^5$ K and their velocity $V = 350$ km s^{-1}, and where the ratio of the maximum to the minimum counting rates is $N_{max}/N_{min} = 3$–5.

But the most spectacular variation of the cometosheath plasma flow characteristics occurs at the cometopause, which separates the cometosheath itself, controlled by the solar wind proton flow, from the inner cometary plasma region dominated by slowly moving cometary ions (Gringauz *et al.* 1985, 1986b, c, d, 1987b). This boundary was not theoretically predicted but was discovered on the basis of PLASMAG-1 data from both Vega spacecraft. The existence of the cometopause was confirmed later by the plasma wave experiment APV-N onboard the Vega spacecraft (Savin *et al.* 1986) and by the instruments PICCA and JPA onboard Giotto (Korth *et al.* 1985, Amata *et al.* 1986).

The top panel of Fig. 13 (Galeev *et al.* 1987) shows the ion spectrogramm measured by the CRA of the PLASMAG-1 package in the vicinity of the cometopause. The outermost isolines correspond to a count rate of 10^3 s^{-1}, and the ratio between count rates represented by adjacent isolines is two. The two vertical dashed lines indicate the time interval 0643–0645 UT when Vega-2 crossed the cometopause (Gringauz *et al.* 1986c).

As shown by the spectrogram of Fig. 13, the typical energy/charge ratio of ions detected by the CRA significantly increases at the cometopause from ~170 eV to ~900 eV. This feature is due to changes in the distribution function and ion composition of the plasma; protons ($m_p = 1$ amu) are most abundant in the cometosheath, while water group ions ($m_i \approx 16$–18 amu) dominate inside the cometopause. Proton fluxes detected by the CRA significantly decrease after crossing the cometopause, though their energy spectra become wider (Gringauz *et al.* 1985, 1986c) and their typical energy increases to ~250 eV.

Before crossing the cometopause, the ion energy spectra observed by the SDA show two maxima (see Figs 9, 10b). The first maximum, which is essentially due to protons is typically ~300 eV; the heavy water group ions produce a second maximum at ~900 eV. After crossing the cometopause, protons practically disappear from the acceptance angle of the SDA, while the energy of heavy ions is hardly changed

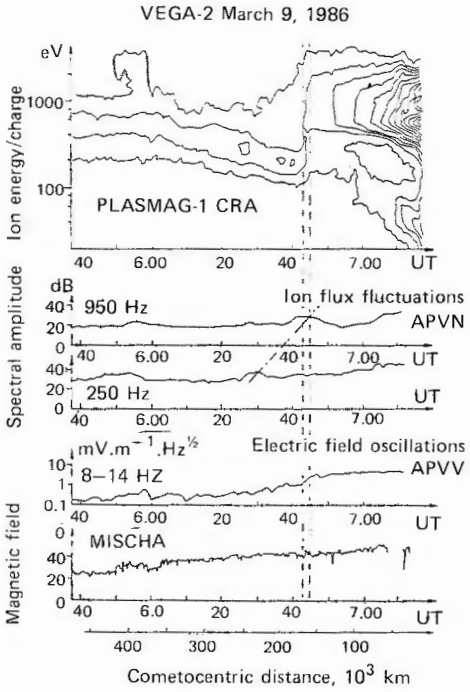

Fig. 13 — Plasma and field data collected by four different instruments during the last 100 min before closest approach. From top to bottom: spectrogram of ion flux in the ram direction, plasma wave activity in three different frequency ranges, total magnetic field. The cometopause is indicated by dashed lines.

(Gringauz *et al.* 1985, 1986c).

Electron spectra measured by the Electron Analyzer, and hence the density and temperature of the electrons, do not show any characteristic variation when the cometopause is crossed (Gringauz *et al.* 1985, 1986c).

Magnetic field measurements performed by the magnetometer MISCHA on board Vega-2 are also consistent with the conclusion that the plasma density does not change significantly at the cometopause. As seen from the bottom panel of Fig. 13, the magnitude of the total magnetic field is practically constant in this region. Only minor changes are observed in the B_y and B_z components (Reidler *et al.* 1985).

The middle part of Fig. 13 shows the plasma wave activity measured by the instruments APV-N and APV-V on board Vega-2. In general, the filter channels shown in this figure (and also other channels not shown here) are characterized by an increase of the average amplitude of plasma and electric

field oscillations from a cometocentric distance of 1.5–2 × 10^5 km when the Vega-2 spacecraft approaches the nucleus. In the vicinity of the cometopause (around 0630–0650 UT), plasma wave oscillations are observed in the whistler frequency range (0.2–1 kHz) and the amplitude of the electric field suddenly increases in the lower hybrid frequency range (8–14 Hz) during a 2 min interval when the spacecraft crosses the cometopause.

The wave activity in the lower frequency range can be seen in Fig. 14 (Galeev *et al.* 1987) where more detailed measurements of plasma, magnetic field, and waves are presented. The top panel shows the ion spectrogram measured by the CRA. Here the difference between count rates represented by adjacent isolines is 440 s^{-1}, and the outermost isolines correspond to a count rate of 10^3 s^{-1}. Dots on the spectrogram mark the maxima of the ion flux in an interval of 10 min around the cometopause. A comparison between the spectrograms simultaneously measured by the CRA and SDA (see Fig. 1 in Gringauz 1986c, where the spectrograms are colour coded) shows that the fluctuations of ion fluxes measured by the two sensors are in anticorrelation. This is an indication of the existence of large-scale MHD variations in the direction and/or in the velocity of the plasma flow with a characteristic period $T \approx 1$ min.

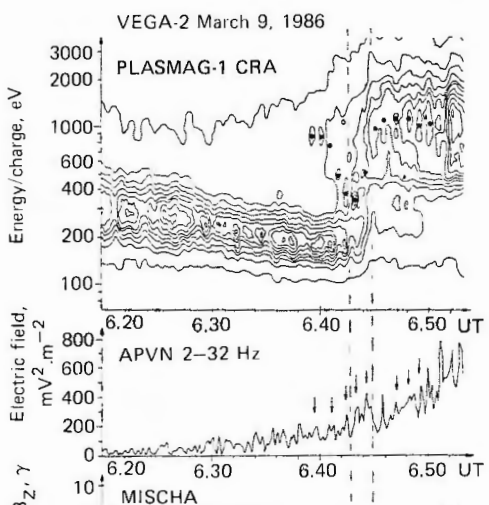

Fig. 14 — Fluctuations of ion flux, electric field and B_z component (pointing toward the north pole of the ecliptic) of the magnetic field around the cometopause (indicated by dashed lines). Maxima are shown by dots and arrows.

These large-scale MHD waves at the cometopause are reflected in the electric field by oscillations at the lower hybrid frequency (2–32 Hz) and in the B_z component of the magnetic field by fluctuations with the same characteristic period ($T \approx 1$ min). The correspondence between the maxima of electric field, magnetic field, and ion fluxes is indicated by arrows in Fig. 14.

The sudden decrease of proton fluxes within a ≈ 2 min interval (corresponding to $\Delta \approx 10^4$ km along the trajectory of Vega-2) in the ram and solar direction cannot be explained without taking into account collisionless deceleration processes and isotropization of the proton distribution function; this phenomenon may be caused by an instability due to the relative motion of solar wind protons and cometary ions. We shall therefore estimate the velocity of the protons and ions observed by PLASMAG-1.

Outside the cometopause, the typical energy of solar wind protons is ~170 eV in the ram direction and ~300 eV in the solar direction. Their estimated bulk velocity relative to the spacecraft is $v_{pr} \approx 250$ km s^{-1}. The velocity of the protons relative to the comet $v_p \approx 200$ km s^{-1} is given by a possible vector diagram shown by Fig. 15 (Galeev *et al.* 1987), where the spacecraft velocity relative to the comet $v_{sc} \approx 80$ km s^{-1} taken into account. Fig. 15 also shows the acceptance angles of the CRA and SDA sensors and the regions of velocity space in which protons can be observed by these analyzers (areas shaded with vertical lines). In a similar way, the velocity of heavy cometary ions can be estimated; $v_{ir} \approx 120$ km s^{-1} relative to the spacecraft, and $v_i \approx 60$ km s^{-1} relative to the comet.

The measured magnetic field direction is not far from parallel to the plasma flow, and a 'fire-hose' instability might develop. Outside the cometopause, when the proton number density is $n_p \approx 10$–20 cm^{-3} and the magnitude of the magnetic field is $B \approx 40\gamma$, the condition for a fire-hose instability caused by the solar wind flow through the cometary plasma is not

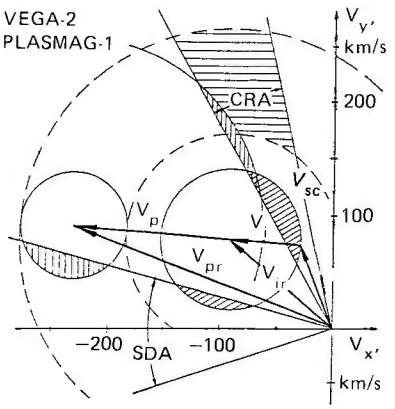

Fig. 15 — Possible proton and ion velocity vector diagrams and the acceptance angles of the SDA and CRA ion analyzers in the spacecraft reference frame. Particles from the shaded areas can be observed by the analyzers (sloping lines: cometary ions, vertical lines: protons outside the cometopause, horizontal lines: protons inside the cometopause).

fulfilled. On the other side of this boundary, when the number density of heavy ions is $n_i \approx 10$ cm^{-3} and the velocity is $v_i \approx 60$ km s^{-1} relative to the comet, the increasing ionization of cometary neutrals leads to an instability caused by the flow of solar wind protons and picked-up cometary ions relative to the newly ionized cometary gas. As a consequence, protons are decelerated, and pitch angle scattering takes place; the intensity of proton fluxes detected by both CRA and SDA is therefore decreasing.

A clear indication of the instability which develops near the cometopause is the large-scale variation of the plasma flow correlated with the oscillations of the perpendicular magnetic field component (relative to the main field direction), as seen in Fig. 14. The characteristic scale of these oscillations is $v_{sc}T \approx 5000$ km along the spacecraft trajectory which is comparable with the thickness of the cometopause Δ, but it is much larger than the Larmor radius of cometary ions $Q_{ci} = v_i/\omega_{ci} \approx 300$ km ($\omega_{ci} \approx 0.2$ s^{-1} is the cyclotron frequency of water group ions). The plasma velocity vector was not measured by the Vega spacecraft, and it is not possible to determine the mode of oscillation excited by the instability. Since the magnitude of the magnetic field is almost constant there, the oscillations seem to be perpendicular. The amplitude of the velocity perturbation δv can be estimated from the oscillation of the perpendicular magnetic field component δB,

$$\delta v \approx (\delta B/B) v_A \approx 10 \text{ km s}^{-1} \qquad (8)$$

where $v_A \approx 60$ km s^{-1} is the Alfvén velocity. This effect can induce strong modulations in the ion flows observed by both analyzers. The large scale of these oscillations compared to the ion Larmor radius indicates that these waves are certainly not caused by cyclotron resonance. In other words, we possibly observe the development of a fire-hose instability with a significantly larger growth rate than in the case of a resonance instability (Galeev *et al.* 1987). The source of energy of such an instability is the kinetic energy of the newly born cometary ions relative to the plasma flow; the density of this flow is much larger than the density of the original solar wind proton flow.

The significant decrease of the proton flux at the cometopause and in the cometary plasma region shows the importance of the charge exchange between protons and cometary gas for producing cometary ions here. The characteristic time for charge exchange is,

$$\tau_{ct} \approx (\sigma_{ct} v_p n_n)^{-1} \approx 6 \times 10^3 \text{ s} \qquad (9)$$

where $\sigma_{ct} \approx 2 \times 10^{-15}$ cm^2 is the cross-section for charge exchange, $n_n \approx 4 \times 10^3$ cm^{-3} is the number density of neutral gas in the vicinity of the cometopause at a cometocentric distance $R \approx 1.6 \times 10^5$ km (Remizov *et al.* 1986), and $v_p \approx 200$ km s^{-1} is the velocity of the proton flow outside the cometopause, which is of the same order of magnitude as the proton gyrovelocity inside the cometopause after pitch angle scattering. Since the above estimated τ_{ct} is comparable to the characteristic time of the plasma flow around the comet (of the order of $2R/v_i \approx 5 \times 10^3$ s in the vicinity of the cometopause for a flow velocity $v_i \approx 60$ km s^{-1}), charge exchange is effective in this region.

As a consequence of the existence of a cometary ion beam in the plasma flow, the intensity of plasma waves is increasing in the lower hybrid frequency range at the cometopause (see Figs 13, 14). The growth of this wave is limited by the quasilinear relaxation of the ion beam to a steady state (Formisano *et al.* 1982), and the wave intensity in the lower hybrid range measured by the instruments APV-V (Fig. 13) and APV-N (Fig. 14) is in reasonable agreement with the theoretical estimate (Galeev *et al.* 1987).

The excited lower hybrid waves accelerate the suprathermal electrons which are in Čerenkov resonance (Galeev & Khabibzachmanov 1985). If the lifetime of the suprathermal electrons was significantly larger than the time of acceleration, their maximum density would be determined by the condition that the electron Landau damping be small compared to the growth rate of the instability. The acceleration of suprathermal electrons along the magnetic field lines leads to the excitation of oblique Langmuir waves (whistlers in high β plasma) due to the growing anisotropy in the velocity distribution of electrons. The frequency of high-frequency Langmuir waves increases as the plasma is decelerating in the vicinity of the cometopause because the energy of suprathermal electrons is decreasing. This effect is marked by a dashed-dotted line in Fig. 13. The increase in the level of lower hybrid and whistler mode plasma oscillations is a consequence of the rapid mass-loading and deceleration of the solar wind by cometary ions in the vicinity of the cometopause. It is not responsible for the mass-loading process (Galeev *et al.* 1987).

3.3 Cometary plasma region and unsteady phenomena

After crossing the cometopause, during the further approach to the cometary nucleus, the CRA sensor observed an increase of the counting rates of heavy cometary ions by an order of magnitude (see, for example, Figs. 13, 14). However, the increase of cometary plasma density was neither monotonic nor stationary. This is shown in Fig. 16 (Gringauz *et al.* 1986d, 1987b) exhibiting two high-resolution spectrograms, as observed during 0700–0704 UT and during 0706–0710 UT, or at distances of about 8×10^4 km and 5×10^4 km, respectively (time runs from right to left). The counting rates corresponding to the outermost lines are given by $f_o = 4 \times 10^3$ s^{-1} and $f_o = 10^4$ s^{-1}, respectively. The increase in the counting rates is characterized in steps of df between two adjacent isolines with d$f = 4 \times 10^2$ s^{-1} and d$f = 10^3$ s^{-1} respectively. From these figures it readily follows that a quasiperiodic modulation in the intensity of cometary ions exists. This modulation is most pronounced in the energy-over-charges range around 500–600 eV, which corresponds to ions of the water group. The typical normalized amplitude (A) in the modulation of these latter ions is about,

$$A = (f_{max} - f_{min})/(f_{max} + f_{min}) \approx 0.05\text{–}0.1$$

Moreover, we find that the modulation period τ_M decreases when approaching the nucleus from about $\tau_M \approx 10$ s at 8×10^4 km to about $\tau_M \approx 8$ s at 5×10^4 km.

It should be noted that this type of modulation differs from the sporadic, burst-type density enhancements which have been observed by Vega-2 at about 4×10^4 km and 3×10^4 km (see Fig. 4 in Gringauz *et al.* 1985). These bursts were associated with enhancements in the plasma wave intensity around the lower hybrid frequency, and their occurrence was possibly connected with the critical ionization velocity effect of Alfvén (Galeev *et al.* 1986).

The observed quasiperiodic modulation in the heavy ion density in the cometary plasma region could be explained by the development of the large-scale instability caused by the anisotropic velocity distributions of cometary ions. This instability is connected with the cyclotron resonance of ions by Alfvén oscillations, therefore the wavelength of these oscillations can be estimated as $\lambda \approx v_\parallel/f_{ci}$ where f_{ci} is the cyclotron frequency of the ions and $v_\parallel$ is their velocity along the magnetic field. Taking the magnetic field of $B \approx 50\gamma$ and the spatial dimensions of the plasma flow fluctuations as ~ 8 s $\times$ 80 km s^{-1} $\approx$ 640 km into account, the field-aligned velocity can be estimated as $v_\parallel \approx 30$ km s^{-1} which seems to be reasonable.

Well inside the cometary plasma region both the thermal and the bulk velocities of ions become small compared to the spacecraft relative velocity of ≈ 80 km s^{-1}. The energy-over-charge spectra break up in several well-defined sub-distributions with their maximum intensity located at distinct E_i/q values. This situation is depicted in Fig. 17 (Gringauz *et al.* 1986d, 1987b), showing a sequence of 4 s averaged ion energy spectra as obtained by the CRA sensor at a distance of $1.4\text{–}1.7 \times 10^4$ km from the nucleus. From the left-hand distribution it readily follows that the bulk velocity of the protons is close to the spacecraft relative velocity. Thus, the energy/charge E_i/q spectra can be transformed into mass/charge m_i/q spectra.

In this way Fig. 17 suggests the presence of H^+, C^+, CO^+_2, and Fe^+ ions in the cometary plasma region. The peak at $14 < m_i/q < 20$ may originate from the

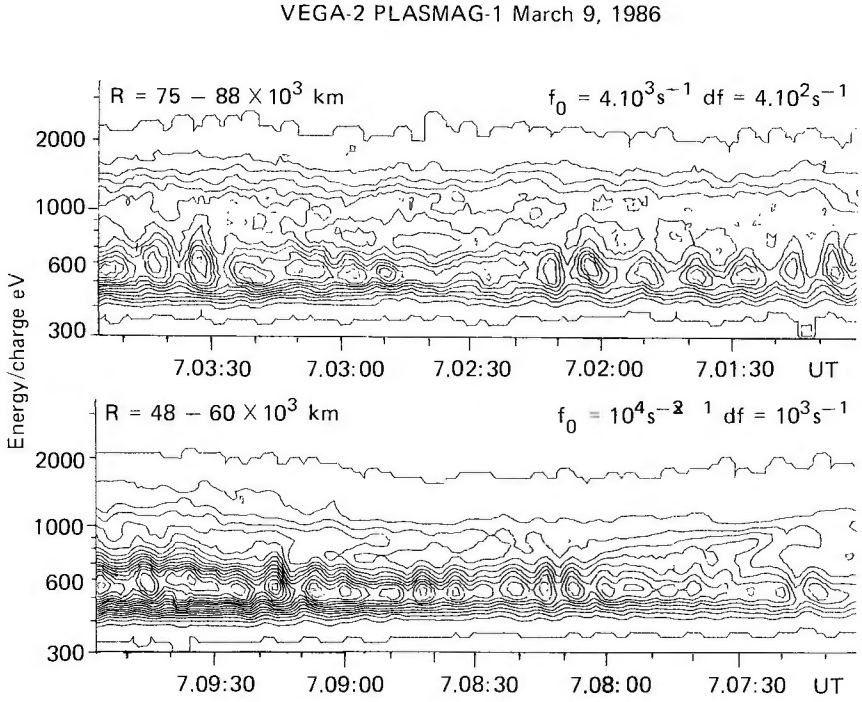

Fig. 16 — Contour plots of the ion intensity vs. energy/charge and time as measured by the CRA on board Vega-2 in the cometary plasma region at distances of 8 × 10^4 km and 5 × 10^4 km from the nucleus.

H_2O parent molecules, such as O^+, OH^+, H_2O^+, and H_3O^+, while the peak at $24 < m_i/q < 34$ may be due to parent molecules of CO/CO_2 or to molecules containing N/S, such as CO^+, N_2^+, H_2CO^+, HCO^+, CN^+, HCN^+, or O_2^+ or to atomic ions like Mg^+, Al^+, Si^+, P^+, or S^+. Finally, the minor peaks at m_i/q = 2, 8, 70, and 85 might stem from H^+_2 and O^{++} and from some heavier, not yet identified organic ions. We have marked these different groups of cometary ions at the top of Fig. 17.

For these groups we have determined their densities at different cometocentric radial distances by summing the respective count rates. The result is shown in Fig. 18 (Gringauz *et al.* 1986d, 1987b), together with the total sum Σ of all ions and with the expected R^{-2} slope. Straight lines correspond to the regions where the densities could be determined more accurately. From Fig. 18 it readily follows that, in principle, really none of the curves, except may be the curve of mass-group 70^+, can be approximated by a pure R^{-2} dependence. For the total sum we find a dependence of $R^{-2.4}$ for 3 × 10^4 < R < 1.5 × 10^4 km.

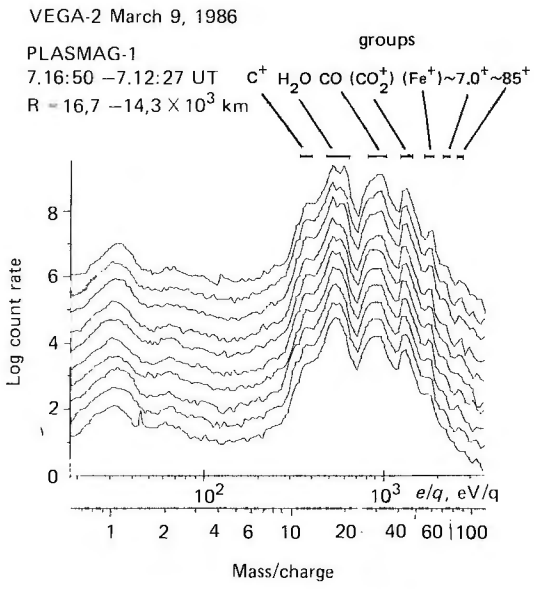

Fig. 17 — Time sequence of 4s averaged ion energy/charge (mass/charge) spectra, as observed by the CRA sensor on board Vega-2 at a cometocentric distance of (1.4–1.7) × 10^4 km.

A somewhat unexpected result is the observed well defined peak at $m_i/q = 56$ in the CRA ion spectra. This peak was also identified in the IMS (Balsiger *et al.* 1986) and NMS (Krankowsky *et al.* 1986) measurements onboard Giotto. However, it has not been observed by the Giotto-PICCA instrument (Korth *et al.* 1986), although otherwise this sensor is quite similar to the CRA sensor onboard Vega-2. It seems quite natural to identify this peak with the occurrence of Fe^+ ions in the innermost part of the cometary plasma region, although it should be noticed that, owing to the energy resolution of the CRA sensor of 5.5%, there is an uncertainty of about 3 amu in the mass resolution. From the observed mass composition of cometary dust particles, iron has been identified in most of the mass spectra analyzed (Kissel *et al.* 1986). Thus, sputtering of dust grains with large metallic cores and no layer of ice could account for the release of metallic ions in the cometary coma, (Ip & Axford 1986) although other processes discussed in (Geiss *et al.* 1986) could also account for the occurrence of metal ions.

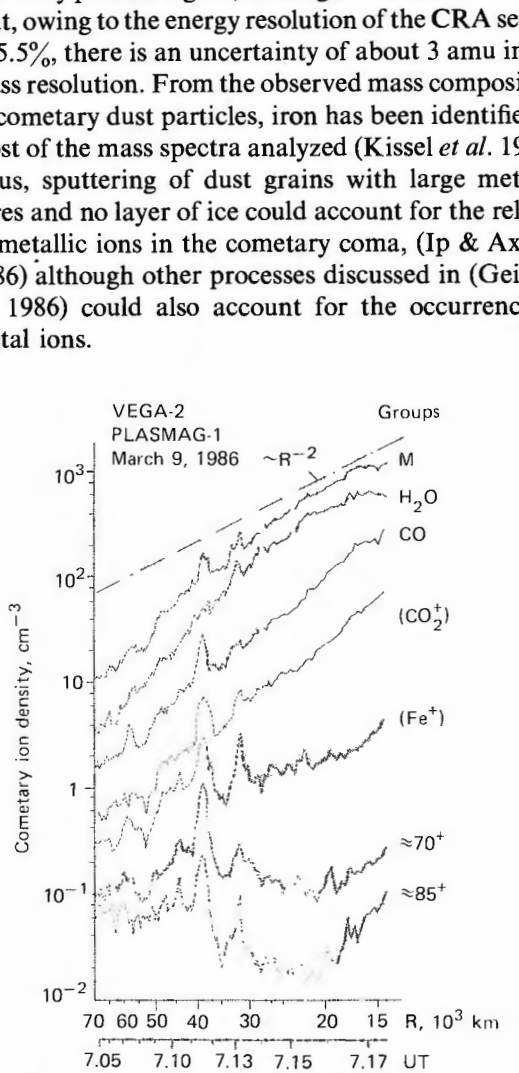

Fig. 18 — Cometocentric radial dependence of the densities of certain groups of cometary ions, as defined in Fig. 17 and of the total sum Σ of all ions. For comparison the R slope is inserted.

As indicated in Fig. 18, the density of cometary ions decreases somewhat faster than R^{-2}. This result is consistent with the observations of the IMS (Balsiger *et al.* 1986) and the PICCA instrument (Korth *et al.* 1987) onboard Giotto. The neutral gas density, however, decreases as R^{-2}, as observed both by Vega (Gringauz *et al.* 1985, 1986b, Remizov *et al.* 1986) and by Giotto (Krankowsky *et al.* 1986). This somewhat faster decrease in the ion density could be associated with the fact that the loss rate of ions increases with increasing distances from the nucleus, owing to an increasing convective outflow of the cometary ions. Vega-2 observed a neutral gas density of $n_o \approx 1.5 \times 10^5$ cm^{-3} at 2×10^4 km (Remizov *et al.* 1986). For a characteristic time of ionization of $\tau_i \approx 10^6$ s, the local production rate for ions is $Q_i \approx n_n/\tau_i \approx 0.15$ cm^{-3} s^{-1}. To obtain an ion density of $n_i \approx 10^3$ cm^{-3} at these distances, a value for the velocity of the convective outflow of $V_i \approx Q_i R/n_i \approx 3$ km s^{-1} would be sufficient. This value for V_i is in reasonable agreement with the velocity determined for the water group ions from the IMS measurement onboard Giotto (Balsiger *et al.* 1986).

On the other hand, if the loss of cometary ions is mainly caused by the convective outflow, then the ratios of the densities of the ions and of their parent molecules must be close to each other. In Krankowsky *et al.* (1986) a value of 5% for the CO_2 content relative to the content of H_2O was estimated. From our CRA measurements we find that 70–80% of the total ion content belongs to the water group ions and 2–5% to the ions with $m_i/q \approx 44$ (CO_2^+. In turn, as we find 15–20% for the content of the CO/CO_2 group ions we can estimate the content of the parent molecules H_2O and CO/CO_2 based on our CRA data to be 70–80% and 15–20%, respectively. This agrees with the production rates of H_2O and CO as determined from the UV measurements onboard the IUE spacecraft (Festou *et al.* 1986).

As an example of the large-scale unsteady cometary phenomena, the inhomogenuity formed in the cometary plasma region by the solar wind IMF parameters change can be considered (Verigin *et al.* 1987b). The general feature of the plasma measurements onboard both Vega craft is the absence of any plasma registration by SDA analysers inside the cometopause. However, in case of Vega-1 this sensor

observed a burst, lasting for about 5 min, of ions with energies E_i = 100–1000 eV approximately, near the closest approach to comet Halley, marked in black in Fig. 9. For roughly the same time interval as in Fig. 9, the SDFC sensor observed ion flux coming from the solar direction, which was evaluated as (5–8) × 10^9 cm^{-2} s^{-1} (Verigin *et al.* 1987b). The density of cometary ions by RFC data could only be estimated to a few thousands per cm^3.

Inspecting the evolution of the magnetic field direction along the Vega-1 trajectory, the authors of magnetic measurements concluded that in addition to the global draping of the magnetic field lines around the comet, the portion of the field observed near closest approach is a remnant of the IMF of the previous polarity (Riedler *et al.* 1986, Schwingenschuh *et al.* 1986).

When interacting near closest approach, two portions of magnetic fields of opposite polarities will lead to an X-type reconnection pattern of the magnetic field lines (Fig. 19). The region in which the SDA and SDEC sensors observed the enhanced flux of ions is indicated by dots in this diagram. It seems

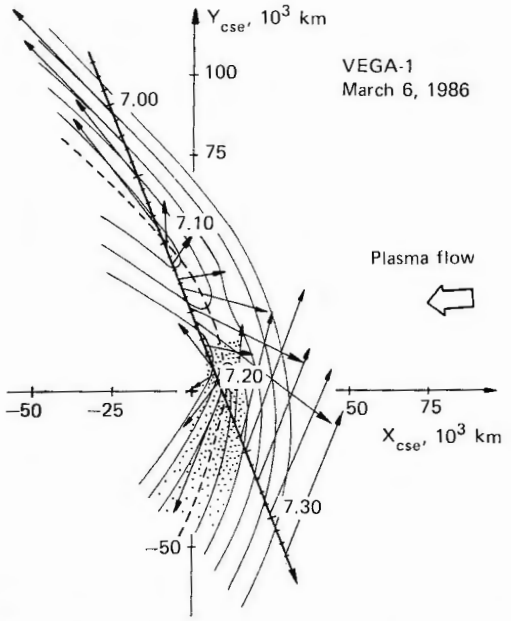

Fig. 19 — Overall topology of the magnetic field around closest approach as deduced from the measurements of the magnetic field direction (arrows) along the Vega-1 trajectory. The dotted areas represents the region in which the burst of accelerated ions (see Fig. 5) was observed.

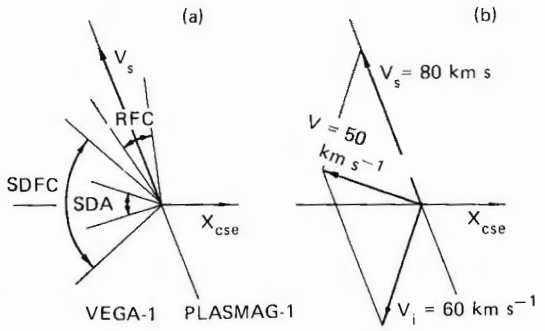

Fig. 20(a) — Schematic representation of the look-directions and the fields of view of the SDA, SDFC, and RFC sensors on board Vega-1 relative to the cometary nucleus and to the spacecraft velocity direction V.

Fig. 20(b) — Vector diagram of the spacecraft velocity V_s and of the ion velocities V_i and V in the cometary frame and in the spacecraft frame of reference, respectively. V_i is presumed to be roughly parallel to the magnetic field lines. Only for large values of $V_i \gtrsim 35$ km^{-1} will ions be detected by the SDFC/SDA sensors, as in this case V will fall into the field-of-view of the SDA/SDFC sensors.

quite reasonable to suggest that these ions were accelerated by the non-stationary process of magnetic field reconnection near closest approach (Verigin *et al.* 1987b).

Why are these ions then observed by the SDA/SDFC sensors only on the outbound leg of the Vega-1 trajectory, not on the inbound leg? The answer is provided by Fig. 20a,b (Verigin *et al.* 1987b). Here, together with look-directions and the angular fields of view of the SDA, SDFC, and RFC sensors (Fig. 20a), the possible diagram of the velocity vectors V_s, V_i, and V is shown. Here, V_s is the velocity of ions at rest in the cometary frame of reference, V_i is the velocity of accelerated ions in the same frame, and $V = V_i + V_s$ is their velocity in the Vega-1 frame of reference. This diagram holds for the outbound situation (V_i is supposed to be parallel to the surface separating magnetic fields of opposite direction which are marked by the dashed curve in Fig. 19). For the inbound case the direction of V_i is close to the direction of V_s, hence the direction of V is close to the same direction (and out of the field of view of SDA/SDFC).

From ion composition measurements (Gringauz *et al.* 1986d, 1987b, Balsiger *et al.* 1986) we know that cometary ions are predominantly the water-group ions with m_i = 16–18. At their velocity relative to Vega-1 of about 50 km s^{-1} (see Fig. 20), they will be observed

at energies $E_i > 200$ eV by the SDA analyzer. This is in agreement with the actual measurements shown in Fig. 6. From the SDFC measurements we estimated the total ion flux as (5–8) $\times 10^9$ cm^{-2} s^{-1}. Taking now their velocity V relative to the spacecraft into account, we are able to estimate their density as $n_i > (1–2) \times 10^3$ cm^{-3}. This value agrees roughly with the number density estimated from the RFC observations.

Based on these different, yet self-consistent, observations we may, in summary, conclude that the burst of cometary ions observed by the SDA and SDFC sensors onboard Vega-1 near closest approach to comet Halley was produced by the motion of cometary ions of the water-group accelerated up to some tens of km s^{-1} (Verigin *et al.* 1987b). This acceleration could be caused by merging of interplanetary magnetic field lines of opposite polarity retarded by the presence of cometary plasma and neutrals.

3.4 The aurora-like phenomena in the vicinity of cometary nucleus

The only essential difference between Vega and Giotto plasma observations within the cometary plasma region is the observation of keV electrons onboard Vega-2 during its closest approach to Comet Halley. Fig. 21 (Gringauz *et al.* 1985, 1986b) presents two typical electron spectra as measured by the EA in the solar wind and near the closest approach of Vega-2 to the cometary nucleus. The main difference between these spectra is the appearance of the energetic

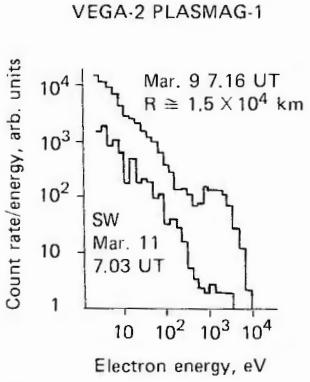

Fig. 21 — Two electron spectra, as measured by the Vega-2 electron analyzer in the solar wind and near closest approach to the cometary nucleus at $\sim 1.5 \times 10^4$ km respectively. Notice the occurrence of keV electrons close to the nucleus.

cometary electron component, which could serve as an additional source of ionization of cometary neutrals.

The presence of ~ 1 keV electrons during the Vega-2 flyby and the absence of similar electrons during the Giotto flyby could be due to either an instrumental effect, or to the sporadic occurrence of these particles. The possible instrumental effect was discussed in Gringauz *et al.* (1986e, 1987a). The electrons with energies of about 1 keV could be generated by a 'magnetospheric substorm', similar to the auroral events occurring in the terrestrial magnetosphere. The occurrence of such events in the cometary magnetotail has been proposed by Ip (1976) and Ip & Mendis (1976). A schematic representation of a 'cometary substorm', as suggested by Ip & Axford (1982) and Mendis *et al.* (1985) is shown in Fig. 22 (Gringauz *et al.* 1986e, 1987a). In the steady state the cometary tail electric current adopts the usual Θ-shape configuration. If the cross-trail current becomes partly disrupted, the induced tail-aligned currents can discharge through the cometary coma (Fig. 22). Such a process can accelerate electrons to energies of a few keV, as in the case of auroral electrons in the terrestrial upper atmosphere. Vega-2 might have observed such substorm generated energetic electrons, while Giotto might not.

We now summarize other observations that point also toward the possibility that energetic electrons may occur sporadically in the coma of Comet Halley. In Feldmann *et al.* (1986) the two UV spectra measured by IUE on 18–19 March 1986, on the tailward side of the nucleus at a distance of about 40 000 km and about 30 min apart, were compared. It was found that the CO_2^+ emission had decreased to less than a quarter, while the OH^+ brightness had remained nearly constant. The authors proposed that this difference could be explained by the existence of localized currents of energetic electrons close to the nucleus.

The far-UV observations of Comet Halley in February 1986 with a sounding rocket experiment showed the presence of $\lambda = 153.6$ nm line tentatively identified as oxygen emission (Woods *et al.* 1986a). This intercombination line is not excited by solar fluorescence as the other emissions are, and it suggests the presence of a region of electron excitation within

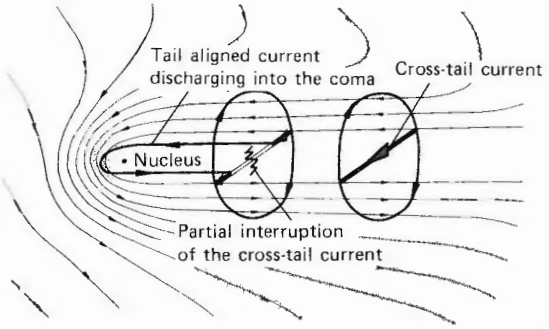

Fig. 22 — Schematics of a cometary cross-tail disruptive event, which could have produced the keV energetic electrons observed by Vega-2 during closest approach (see Fig. 21).

the inner coma (Woods *et al.* 1986a). The consideration of a collisional processes with the electrons helps toward the solution of the 'carbon puzzle' (Woods *et al.* 1986), which is connected with the presence of unexpectedly large amount of neutral and ionized carbon in the vicinity of P/Halley and other comets (Balsiger *et al.* 1986, Festou 1984).

4 CONCLUSIONS

The results of *in situ* neutral and plasma measurements during the Vega-1, 2 encounters with P/Halley which have been presented above, generally confirmed the MHD description of the solar wind interaction with cometary plasma (see, for example, Ip & Axford 1982), yet led to the discovery of a number of phenomena that were not envisaged by the existing theories.

In accordance with the predictions:

- the deceleration of the solar wind flow due to mass loading starts a few million kilometres from the nucleus;
- the bow shock is formed near $R \approx 10^6$ km, although the possibility of the absence of this structure is also discussed;
- the additional solar wind mass loading by cometary ions and the associated increases of plasma pressure and density leads to the very low velocities of the flow at $R \lesssim 10^5$ km;
- some evidences of the 'substorm' phenomenon in the cometary magnetosphere were obtained.

On the other hand:

- the distribution function of the multicomponent plasma within the cometosheath and the cometary plasma region turned out to be a stable but essentially unequilibrium function — there are two branches of the picked-up cometary ions in the cometosheath. The protons and the heavy ions in the cometary plasma region seem to be decoupled;
- the existence of the cometopause — the relatively sharp, yet unpredicted boundary within the cometary coma at cometocentric distances of about 1.6×10^5 km — was revealed;
- the continuous cooling of the electron plasma component through the cometosheath, due to inelastic collisions with neutrals, was observed;
- it was shown that the increase of heavy ion densities within the cometary plasma region is not monotonic but lumpy, quasiperiodic, with a 'period' decreasing while approaching the nucleus;
- the unexpected presence of Fe^+ ions in the P/Halley plasma was demonstrated.

These and a number of other peculiarities of near-cometary plasma are not yet finally and quantitively analyzed. There are new possibilities for such studies on the basis of the qualitative analyses of the data obtained.

REFERENCES

Amata, E., Formisano, V., Cerulli-Irelli, R., Torrente, P., Johnstone, A.D., Wilken, B., Jockers, K., Winningham, J.D., Bryant, D., Borg, H., & Thomsen, M. (1986) The cometopause region at Comet Halley, In: *Exploration of Halley's Comet, ESA SP-250* **1** 213–218

Apáthy, I., Remizov, A.P., Gringauz, K.I., Balebanov, V.M., Szemerey, I., Szendrö, S., Gombosi, T., Klimenko, I.N., Verigin, M.I., Keppler, E., & Richter, A.K. (1986) Plasmag-1 experiment: solar wind measurements during the closest approach to Comet Giacobini–Zinner by the ICE probe and to Comet Halley by Giotto and Suisei spacecraft, In: *Exploration of Halley's Comet, ESA SP-250* **1** 65–70

Balsiger, H., Altwegg, K., Bühler, F., Geiss, J., Ghielmetti, A.G., Goldstein, B.E., Goldstein, R., Huntress, W.T., Ip W.-H., Lazarus, A.J., Meier, A., Neugebauer, M., Rettenmund, U., Rosenbauer, H., Schwenn, R., Sharp, R.D., Shelley, E.G., Ungstrup, E., & Young, D.T. (1986) Ion composition and dynamics at Comet Halley, *Nature* **321** 330–334

Balebanov, V.M., Gringauz, K.I., Verigin, M.I. (1987) Plasma phenomena in the vicinity of the closest approach of VeGa-1,-2 spacecraft to the Halley Comet nucleus, In: *Symposium on diversity and similarity of comets, ESA SP-278*, 119–127

Feldman P.D., A'Hearn, M.F., Festou M.C., McFadden L.A., Weaver H.A., & Woods T.N. (1986) Is CO_2 responsible for the outburst of Comet Halley?, *Nature* **324** 443–436

Festou, M.C. (1984) Aeronomical processes in cometary atmospheres: the carbon compounds puzzle, Adv. Space Res. **4**, No. 9, 165–175

Festou, M.C., Feldman, P.D., A'Hearn, M.F., Arpigny, C., Cosmovici, C.W., Danks, A.C., McFadden, L.A., Gilmozzi, R., Patriarchi, P., Tozzi, G.P., Wallis, M.K., & Weaver, H.A. (1986) IUE observations of Comet Halley during the Vega and Giotto encounters, *Nature* **321** 361–363

Formisano, V., Galeev, A.A., & Sagdeev, R.Z. (1982) The role of critical ionization velocity phenomena in the production of inner coma cometary plasma, *Planet. Space Sci* **30** 791–797

Galeev, A.A. (1985) Solar wind interaction with Comet Halley, *Adv. Space Res* **5** No. 12, 155–163

Galeev, A.A. (1986) Theory and observations of solar wind/cometary plasma interaction processes, In: *Exploration of Halley's Comet, ESA SP-250* **1** 3–17

Galeev, A.A. (1987) Encounters with comets: Discoveries and puzzles in cometary plasma physics, *Astron. Astrophys* **187** 12–20

Galeev, A.A. & Khabibzachmanov, I.Kh. (1985) On the nature of plasma waves in the Io torus, *Letters Astron. J.*, (in Russian) **11** 292–297

Galeev, A.A., Gribov, B.E., Gombosi, T., Gringauz, K.I., Klimov, S.I., Oberz, P., Remizov, A.P., Riedler, W., Sagdeev, R.Z., Savin, S.P., Sokolov, A.Yu., Shapiro, V.D., Shevchenko, V.I., Szegö, K., Verigin, M.I., & Yeroshenko, Ye.G. (1986a) a) Position and structure of the Comet Halley bow shock: Vega-1 and Vega-2 measurements, *Geophys. Res. Lett.* **13** 841–844

Galeev, A.A., Gringauz, K.I., Klimov, S.I., Remizov, A.P., Sagdeev, R.Z., Savin, S.P., Sokolov, A.Yu., Verigin, M.I., & Szegö, K. (1986b) Critical ionization velocity effects in the inner coma of Comet Halley: measurements by Vega-2, *Geophys. Res. Lett.* **13** 845–849

Galeev, A.A., Gringauz, K.I., Klimov, S.I., Remizov, A.P., Sagdeev, R.Z., Savin, S.P. Sokolov, A.Yu., Verigin, M.I., Szegö, K., Tátrallyay, M., F Grard, R., Yeroshenko, Ye.G., Mogilevsky, M.J., Riedler, W., & Schwingenschuh, K. (1987) Physical processes in the vicinity of the cometopause interpreted on the basis of plasma, magnetic field and plasma wave data measured on board the Vega-2 spacecraft, In: *Symposium on diversity and similarity of comets. ESA SP-278.* 83–87

Geiss, T., Boshler, P., Ogilvie, K.W., & Caplan, M.A. (1986) Origin of metal ions in the coma of P/Giacobini–Zinner, *Astron. Astrophys* **166** L1–L4

Gringauz, K.I., Apáthy, I., Denshikova, L.I., Gombosi, T., Keppler E., Klimenko, I.N., Remizov, A.P., Richter, A.K., Skuridin, G.A., Somogyi, A., Szabó, L., Szemerey, I., Szendrö, S., Verigin, M.I., Vladimirova, G.A., & Volkov, G.I. (1983) The Vega probe instrument package for measuring charged particles with energies less than 25 keV, In: *Cometary exploration* III, Budapest, Central Res. Inst. Phys. Press., 333–350

Gringauz, K.I., Gombosi, T.I., Remizov, A.P., Apáthy, I., Szemerey, I., Verigin, M.I., Denchikova, L.I., Dyachkov, A.V., Keppler, E., Klimenko, I.N., Richter, A.K., Somogyi, A.J., Szegö, K., Szendrö, S., Tátrallyay M., Varga, A., & Vladimirova, G.A., (1985) First Results of plasma and neutral gas measurements from Vega 1/2 near Comet Halley, *Adv. Space Res* **5** 12, 165–174

Gringauz, K., Klimenko, I., Remizov, A., Verigin, M., Vladimirova, G., Apáthy, I., Szegö, K., Szemerey, I., Szendrö, S., Tátrallyay, M., Keppler, E., & Richter, A. (1986a) The Vega Plasmag-1 experiment: description and first results, In: *Field, particle and wave experiments on cometary missions*, Graz, Austrian Academy of Sciences Publication, 203–216

Gringauz, K.I., Gombosi, T.I., Remizov, A.P., Apáthy, I., Szemerey, I., Verigin, M.I., Denchikova, L.I., Dyachkov, A.V., Keppler, E., Klimenko, I.N., Richter, A.K., Somogyi, A.J., Szegö, K., Szendro, S., Tátrallyay, M., Varga, A., & Vladimirova, G.A., (1986b) First *in situ* plasma and neutral gas measurements at Comet Halley, *Nature* **321** 282–285

Gringauz, K.I., Gombosi, T.I., Tátrallyay, M., Verigin, M.I., Remizov, A.P., Richter, A.K., Apáthy, I., Szemerey, I., Dyachkov, A.V., Balakina, O.V., & Nagy, A.F. (1986c) Detection of a new 'chemical' boundary at Comet Halley, *Geophys. Res. Lett*, **13** 613–616

Gringauz, K.I., Verigin, M.I., Richter, A.K., Gombosi, T.I., Szegö, K., Tátrallyay, M., Remizov, A.P., & Apáthy, I. (1986d) Cometary plasma region in the coma of Comet Halley: Vega-2 measurements, In: *Exploration of Halley's Comet, ESA SP-250* **1** 93–97

Gringauz, K.I., Remizov, A.P., Verigin, M.I., Richter, A.K., Tátrallyay, M., Szegö, K., Klimenko, I.N., Apáthy, I., Gombosi, T.I., & Szemerey T. (1986e) Electron component of the plasma around Halley's Comet measured by the electrostatic electron analyzer of PLASMAG-1 on board Vega-2, In: *Exploration of Halley's Comet, ESA SP-250* **1** 195–198

Gringauz, K.I., Remizov, A.P., Verigin, M.I., Richter, A.K., Tátrallyay, M., Szegö, K., Klimenko, I.N., Apáthy, I., Gombosi, T.I., & Szemerey, T. (1987a) Analyses of electron measurements from the PLASMAG-1 experiment on board Vega-2 in the vicinity of Comet Halley, *Astron. Astrophys.* **187** 287–289

Gringauz, K.I., Verigin, M.I., Richter, A.K., Gombosi, T.I., Szegö, K., Tátrallyay, M., Remizov, A.P., & Apáthy, I. (1987b) Quasi-periodic features and the radial distribution of cometary ions in the cometary plasma region of Comet Halley, *Astron. Astrophys.* **187** 191–197

Ip W.-H. (1976) Currents in cometary atmosphere, *Planet. Space Sci.* **27** 121–125

Ip W.-H. & Axford W.I. (1982) Theories of physical processes in the cometary comae and in ion tails, In: *Comets*, ed. L.L. Wilkening, Univ. of Arizona Press, Tucson, Arizona, 588–634

Ip W.-H., & Axford W.I. (1986) Metallic ions in cometary comae and plasma tails, *Nature* **321** 682–684

Ip W.-H., & Mendis D.A. (1976) The generation of magnetic fields and electric currents in the cometary plasma tails, *Icarus* **29** 147–151

Johnstone, A., Coates, A., Kellock, S., Wilken, B., Jockers, K., Rosenbauer, H., Studeman, W., Weiss, W., Formisano, V., Amata, E., Cerulli-Irelli, R., Dobrowolny, M., Terenzi, R., Egidi, A., Borg, H., Hultquist, B., Winningham, J., Gurgido, C., Bryant, D., Edwards, T., Feldman, W., Thomsen, M., Wallis, M.K., Biermann, L., Schmidt, H., Lust, R., & Haerendel, G., Paschmann, G. (1986) Ion flow at Comet Halley, *Nature* **321** 344–347

Kaminsky, M., (1965) *Atomic ionic impact phenomena on metal surface*, Springer-Verlag, Berlin

Kissel, J., Brownlee, D.E., Bühler, K., Clark, B.C., Fehtig, H., Grün, E., Hornung, K., Igenbergs, E.B., Jessberger, E.K., Krueger, F.R., Kuczera, H., McDonnell, J.A.M., Monfil, G.M., Rahe, T., Schweur, G.H., Sekanina, Z., Utterback, N.G., Völk, H.J., & Zook, H.A. (1986) Composition of Comet Halley dust particles from Giotto observations, *Nature* **321** 336–337

Korth, A., Richter, A.K., Anderson, K.A., Carlson, C.W., Cartis, D.W., Lin, R.P., Rème, H., Sauvaud, J.A., d'Uston, C., Cotin,

F., Cos, A.,
at and with
Space Res **5**

Korth, A., Rich
C.W., Curti
d'Uston, C.,
spectra of he

Korth, A., Richt
C.W., Curti
Sauvaud, J.A
dependence
Astron. Astr

Krankowsky, D.
Eberhardt,
Berthelier, J
(1986) *In si*
Nature **321**

Krasnopolsky, V
Krysko, A.,
Clairemidi,
Troshin, V.
Comet Hal
Nature **321**

Mendis, D.A.,
physics of c

Moreels, G., Go
Vincent, M
Festou, M.C
Moroz, V.I
ultraviolet
Vega-2, *Na*

Olivero, J.J., S
deposition i
Geophys. Re

Rème, H., Sau
Anderson,
Mendis, D.
Halley — s
aboard Gio

Remizov, A.P.
Szemerey, I
ments of n
Halley by
Exploration

Riedler, W., Sch
V.A., & R
Comet Hal

Sagdeev, R.Z.,
(1986) MH
region, *Geo*

Savin, S., Avan
Oberc, P., C
the plasma
Comet, ES

Schwingenschul
Styashkin,
(1986) Cor
Adv. Space

Shmidt, R., & A
changed se
cometary fi
environmen

F., Cos, A., & Mendis, D.A. (1985) Cometary ion observations at and within cometopause — region of Comet Halley, *Adv. Space Res* **5** No. 12, 221–225

Korth, A., Richter, A.K., Leidl, A., Anderson, K.A., Carlson, C.W., Curtis, D.W., Lin, R.P., Rème, H., Sauvaud, J.A., d'Uston, C., Cotin, F., Cros, A., & Mendis, D.A. (1986) Mass spectra of heavy ions near Comet Halley, *Nature* **321** 335–336

Korth, A., Richter A.K., Mendis D.H., Anderson K.A., Carlson C.W., Curtis, D.W., Lin R.P., Mitchell D.L., Rème, H., Sauvaud, J.A., d'Uston, C., (1987) The composition and radial dependence of cometary ions in the coma of Comet P/Halley, *Astron. Astrophys* **187** 149–152

Krankowsky, D., Lämmerzahl, P., Herrwerth, I., Woweries, J., Eberhardt, P., Dolder, U., Herrmann, U., Schulte, W., Berthelier, J.J., Illiano, J.M., Hodges, R.R., & Hoffman, J.H. (1986) *In situ* gas and ion measurements at Comet Halley, *Nature* **321** 326–329

Krasnopolsky, V.A., Gogoshev, M., Moreels, G., Moroz, V.I., Krysko, A., Gogosheva, Ts., Palazov, K., Sargoichev, S., Clairemidi, J., Vincent, M., Bertaux, J.L., Blamont, J.E., Troshin, V.S., & Valnicek, B. (1986) Spectroscopic study of Comet Halley by the Vega-2 three-channel spectrometer, *Nature* **321** 269–271

Mendis, D.A., Houpis, H.L.F., & Marconi, M.L. (1985) The physics of comets, *Fundam. Cosm. Phys* **10** 1–380

Moreels, G., Gogoshev, M., Krasnopolsky, V.A., Clairemidi, J., Vincent, M., Parisot, J.P., Bertaux, J.L., Blamont, J.E., Festou, M.C., Gogosheva, Ts., Sargoichev, S., Palasov, K., Moroz, V.I., Krysko, A.A., & Vanysek, V. (1986) Near-ultraviolet and visible spectrometry of Comet Halley from Vega-2, *Nature* **321** 271–273

Olivero, J.J., Stagat, R.W., & Green, A.E.S. (1972) Electron deposition in water vapour, with atmospheric application, *J. Geophys. Res.* **77** 4797–4811

Rème, H., Sauvaud, J.A., d'Uston, C., Cotin, F., Cross, A., Anderson, K.A., Carlson, C.W., Curtis, D.W., Lin, R.P., Mendis, D.A., Korth, A., & Richter, A.K. (1986) Comet Halley — solar wind interaction from electron measurements aboard Giotto, *Nature* **321** 349–352

Remizov, A.P., Verigin, M.I., Gringauz, K.I., Apáthy, I., Szemerey, I., Gombosi, T.I., & Richter, A.K. (1986) Measurements of neutral particle density in the vicinity of Comet Halley by Plasmag-1 on board Vega-1 and Vega-2, In: *Exploration of Halley's Comet, ESA SP-250* **1** 387–390

Riedler, W., Schwingenschuh, K., Yeroshenko, Ye.G., Styashkin, V.A., & Russell, C.T. (1986) Magnetic field observations in Comet Halley's coma, *Nature* **321** 288–289

Sagdeev, R.Z., Shapiro, V.D., Shevchenko, V.I., & Szegö, K. (1986) MHD turbulence in the solar wind — comet interaction region, *Geophys. Res. Lett.* **13** 85–88

Savin, S., Avanesov, G., Balikhin, M., Klimov, S., Sokolov, A., Oberc, P., Orlowski, D., & Krawczyk, Z. (1986) ELF waves in the plasma regions near the comet, In: *Exploration of Halley's Comet, ESA SP-250* **3** 433–436

Schwingenschuh, K., Riedler, W., Schelh, G., Yeroshenko, E.G., Styashkin, V.A., Luhman, J.G., Russell, C.T., & Fedder, J.A. (1986) Cometary boundaries: Vega observations at Halley, *Adv. Space Res.* **6** No. 1, 217–268

Shmidt, R., & Azens, A. (1987) Measurements of integral yields of changed secondary particles using neutral beams simulating a cometary flyby, In: *The Giotto spacecraft impact-induced plasma environment, ESA SP-227*, 15–19

Shmidt, H.U., & Wegmann, R. (1982) Plasma flow and magnetic fields in the comets, In: *Comets*, Tucson, Univ. of Arizona Press, 538–634

Verigin, M.I., Gringauz, K.I., Richter, A.K., Gombosi, T.I., Remizov, A.P., Szegö, K., Apáthy, I., Szemerey, I., Tátrallyay, M., & Lezhen, L.A. (1986) Characteristic features of the cometosheath of Comet Halley: Vega-1 and Vega-2 observations In: *Exploration of Halley's Comet, ESA SP-250* **1** 169–173

Verigin, M.I., Gringauz, K.I., Richter, A.K., Gombosi, T.I., Remizov, A.P., Szegö, K., Apáthy, I., Szemerey, I., Tátrallyay, M., & Lezhen, L.A. (1987a) Plasma properties from the upstream region to the cometopause of Comet Halley: Vega observations, *Astron. Astrophys.* **187** 89–93

Verigin, M.I., Axford, W.I., Gringauz, K.I., & Richter, A.K. (1987b) Acceleration of cometary plasma in the vicinity of Comet Halley associated with an interplanetary magnetic field polarity change, *Geophys. Res. Lett.* **14** 987–990

Woods, T.N., Feldman, P.D., Dymond, K.F., Sahnow, D.J. (1986) Rocket ultraviolet spectroscopy of Comet Halley and abundance of carbon monoxide and carbon, *Nature* **324** 436–438

Woods, T.N., Feldman, P.D., & Dymond, D.F. (1986) The atomic carbon distribution in the coma of Comet Halley, In: *Exploration of Halley's Comet, ESA SP-250* **1** 431–435